

Polar Open-Framework Structure, Optical Properties, and Electron Paramagnetic Resonance of the Mixed-Metal Uranyl Phosphate $\text{Cs}_2[\text{UO}_2(\text{VO}_2)_2(\text{PO}_4)_2] \cdot 0.59\text{H}_2\text{O}$

Tatiana Y. Shvareva,[†] James V. Beitz,[‡]
Evert C. Duin,[†] and Thomas E. Albrecht-Schmitt^{*,†}

Department of Chemistry and Biochemistry,
Auburn University, Auburn, Alabama 36849,
and Chemistry Division, Argonne National Laboratory,
Argonne, Illinois 60439

Received September 15, 2005

Revised Manuscript Received October 28, 2005

One of the current challenges in uranium chemistry is the preparation of solids with three-dimensional framework structures for possible applications as selective-oxidation catalysts,^{1–3} nonlinear optical (NLO) materials,^{4,5} ion-exchange materials,⁶ ionic conductors,⁷ and storage materials for radionuclides.⁸ The challenge in this chemistry lies in the fact that most U(VI) compounds are layered.^{9,10} This feature can be ascribed to the terminal nature of the oxo atoms of the uranyl cation that are typically aligned in a parallel fashion within the layers.^{9,10} However, recent work has demonstrated several routes to preparing three-dimensional structures that include the use of octahedral building units (e.g., in the periodates $\text{K}_2[(\text{UO}_2)_2(\text{VO})_2(\text{IO}_6)_2\text{O}] \cdot \text{H}_2\text{O}^4$ and $\text{A}[(\text{UO}_2)_3(\text{HIO}_6)_2(\text{OH})(\text{O})(\text{H}_2\text{O})] \cdot 1.5\text{H}_2\text{O}$ (A = Li – Cs, Ag)¹¹ and in the gallium phosphate $\text{Cs}_4[(\text{UO}_2)_2(\text{GaOH})_2(\text{PO}_4)_4] \cdot \text{H}_2\text{O}^6$) and the use of organic structure-directing agents (e.g., in molybdates $[\text{C}_6\text{H}_{16}\text{N}]_2[(\text{UO}_2)_6(\text{MoO}_4)_7(\text{H}_2\text{O})_2] \cdot (\text{H}_2\text{O})_2^{12}$ and $[(\text{C}_2\text{H}_5)_2\text{NH}_2]_2[(\text{UO}_2)_4(\text{MoO}_4)_5(\text{H}_2\text{O})](\text{H}_2\text{O})^{13}$ and in the fluorophosphate $[\text{C}_6\text{H}_{14}\text{N}_2]_2[(\text{UO}_2)_6(\text{H}_2\text{O})_2\text{F}_2(\text{PO}_4)_2(\text{HPO}_4)_4] \cdot 4\text{H}_2\text{O}^{14}$).

One of the unusual features of some of these compounds is that they adopt acentric structures. The uranyl periodates, $\text{K}_2[(\text{UO}_2)_2(\text{VO})_2(\text{IO}_6)_2\text{O}] \cdot \text{H}_2\text{O}^4$ and $\text{A}[(\text{UO}_2)_3(\text{HIO}_6)_2(\text{OH})(\text{O})(\text{H}_2\text{O})] \cdot 1.5\text{H}_2\text{O}$ (A = Li – Cs, Ag),¹¹ both crystallize in polar space groups, whereas the uranyl molybdates $[\text{C}_6\text{H}_{16}\text{N}]_2[(\text{UO}_2)_6(\text{MoO}_4)_7(\text{H}_2\text{O})_2] \cdot (\text{H}_2\text{O})_2^{12}$, $(\text{UO}_2)_{0.82}[\text{C}_8\text{H}_{20}\text{N}]_{0.36}[(\text{UO}_2)_6(\text{MoO}_4)_7(\text{H}_2\text{O})_2] \cdot (\text{H}_2\text{O})_m^{15}$, $[\text{C}_6\text{H}_{14}\text{N}_2]_2[(\text{UO}_2)_6(\text{MoO}_4)_7(\text{H}_2\text{O})_2] \cdot (\text{H}_2\text{O})_m^{15}$ and $[(\text{C}_2\text{H}_5)_2\text{NH}_2]_2[(\text{UO}_2)_4(\text{MoO}_4)_5(\text{H}_2\text{O})](\text{H}_2\text{O})^{13}$ are all chiral. The noncentrosymmetric nature of these structures allows for the observation of key physical properties including second-harmonic generation (SHG) of laser light. Herein we report on a remarkable open-framework uranyl phosphate, namely, $\text{Cs}_2[(\text{UO}_2(\text{VO}_2)_2(\text{PO}_4)_2) \cdot 0.59\text{H}_2\text{O}$ (**UVP-1**).

The preparation of $\text{Cs}_2[(\text{UO}_2(\text{VO}_2)_2(\text{PO}_4)_2) \cdot 0.59\text{H}_2\text{O}$ (**UVP-1**) was achieved by reacting $\text{UO}_2(\text{NO}_3)_2 \cdot 6\text{H}_2\text{O}$ with V metal, phosphoric acid, and CsCl under mild hydrothermal conditions.¹⁶ This reaction results in the formation of large clusters of yellow crystals with individual crystals exceeding 3 mm in length. The key feature of this reaction is the use of vanadium metal as the source of vanadium.¹⁷

The structure¹⁸ of $\text{Cs}_2[(\text{UO}_2(\text{VO}_2)_2(\text{PO}_4)_2) \cdot 0.59\text{H}_2\text{O}$ (**UVP-1**) consists of uranyl cations bound by phosphate to yield UO_6 tetragonal bipyramids. These units are bridged by phosphate to yield one-dimensional chains that run down the *c* axis. This basic one-dimensional topology is recognized to occur in several uranyl phases including $\text{Cu}_2[\text{UO}_2(\text{PO}_4)_2]$.¹⁹ The uranyl phosphate chains are fused with chains of corner-sharing VO_5 distorted square pyramids that run down the *b* axis into a novel open-framework structure. There are intersecting channels that occur along the *b* and *c* axes as is shown in Figure 1a,b. The channels running down the *b* axis are approximately $5.5 \times 10.9 \text{ \AA}$, whereas those running down the *c* axis are $5.0 \times 9.5 \text{ \AA}$. These channels are occupied by Cs^+ cations and water molecules. One the most apparent

[†] Auburn University.

[‡] Argonne National Laboratory.

- Hutchings, G. J.; Heneghan, C. S.; Hudson, I. D.; Taylor, S. H. *Nature* **1996**, *384*, 341.
- Pollington, S. D.; Lee, A. F.; Overton, T. L.; Sears, P. J.; Wells, P. B.; Hawley, S. E.; Hudson, I. D.; Lee, D. F.; Ruddock, V. *Chem. Commun.* **1999**, *8*, 725.
- Sykora, R. E.; King, J.; Illies, A.; Albrecht-Schmitt, T. E. *J. Solid State Chem.* **2004**, *177*, 1717.
- Sykora, R. E.; Albrecht-Schmitt, T. E. *Inorg. Chem.* **2003**, *42*, 2179.
- Almond, P. M.; Albrecht-Schmitt, T. E. *Inorg. Chem.* **2002**, *41*, 1177.
- Shvareva, T. Y.; Sullens, T. A.; Shehee, T. C.; Albrecht-Schmitt, T. E. *Inorg. Chem.* **2005**, *44*, 300.
- Obbade, S.; Dion, C.; Rivenet, M.; Saadi, M.; Abraham, F. *J. Solid State Chem.* **2004**, *177*, 2058.
- Pichot, E.; Dacheux, N.; Brandel, V.; Genet, M. *New J. Chem.* **2000**, *24*, 1017.
- Burns, P. C.; Miller, M. L.; Ewing, R. C. *Can. Mineral.* **1996**, *34*, 845.
- Burns, P. C. *Can. Mineral.* **2005**, in press.
- Sullens, T. A.; Jensen, R. A.; Shvareva, T. Y.; Albrecht-Schmitt, T. E. *J. Am. Chem. Soc.* **2004**, *126*, 2676.
- Krivovichev, S. V.; Armbruster, Th.; Chernyshov, D. Y.; Burns, P. C.; Nazarchuk, E. V.; Depmeier, W. *Micropor. Mesopor. Mater.* **2005**, *78*, 225.
- Krivovichev, S. V.; Cahill, C. L.; Nazarchuk, E. V.; Burns, P. C.; Armbruster, Th.; Depmeier, W. *Micropor. Mesopor. Mater.* **2005**, *78*, 209.
- Doran, M. B.; Stuart, C. L.; Norquist, A. J.; O'Hare, D. *Chem. Mater.* **2004**, *16*, 565.

- Krivovichev, S. V.; Burns, P. C.; Armbruster, Th.; Nazarchuk, E. V.; Depmeier, W. *Micropor. Mesopor. Mater.* **2005**, *78*, 217.
- $\text{Cs}_2[(\text{UO}_2(\text{VO}_2)_2(\text{PO}_4)_2) \cdot 0.59\text{H}_2\text{O}$, $\text{UO}_2(\text{NO}_3)_2 \cdot 6\text{H}_2\text{O}$ (0.289 g, 0.57 mmol), V (0.059 g, 1.14 mmol), H_3PO_4 (0.169 g, 1.72 mmol), CsCl (0.484 g, 2.85 mmol), and 1 mL of Millipore-filtered water were loaded into the 23 mL autoclave. The reaction was run at 190 °C in a box furnace for 5 days and then cooled at a rate of 9 °C/h to the room temperature. Clusters of bright yellow crystals of $\text{Cs}_2[(\text{UO}_2(\text{VO}_2)_2(\text{PO}_4)_2) \cdot 0.59\text{H}_2\text{O}$ were isolated, washed with methanol, and allowed to dry. Yield, 515 mg (quantitative yield based on U). Energy-dispersive X-ray analysis provided a Cs:U:V:P ratio of 2/1/2/2.
- Calin, N.; Serre, C.; Sevov, S. C. *J. Mater. Chem.* **2003**, *13*, 531.
- (a) X-ray structural analyses: $\text{Cs}_2[(\text{UO}_2(\text{VO}_2)_2(\text{PO}_4)_2) \cdot 0.59\text{H}_2\text{O}$, yellow prism, crystal dimensions $0.169 \times 0.128 \times 0.105 \text{ mm}$, orthorhombic, *Cmc*2₁, *Z* = 4, *a* = 20.7116(14), *b* = 6.8564(5), *c* = 10.5497(7) Å, *V* = 1498.13(18) Å³ (*T* = 193 K), $\mu = 170.76 \text{ cm}^{-1}$, *R*₁ = 0.0265, *wR*₂ = 0.0602. Bruker APEX charge-coupled device diffractometer; $\theta_{\text{max}} = 56.62^\circ$, Mo *K*α, $\lambda = 0.71073 \text{ \AA}$, $0.3^\circ \omega$ scans, 6369 reflections measured, 1811 independent reflections, all of which were included in the refinement. The data were corrected for Lorentz-polarization effects and for absorption, solutions were solved by direct methods, anisotropic refinement of *F*² was by full-matrix least-squares, and there were 105 parameters. (b) Sheldrick, G. M. *SHELXL PC*, Version 6.12; an integrated system for solving, refining, and displaying crystal structures from diffraction data; Siemens Analytical X-Ray Instruments, Inc.: Madison, WI, 2001.
- Guesdon, A.; Charon, J.; Provost, J.; Raveau, B. *J. Solid State Chem.* **2002**, *165*, 89.

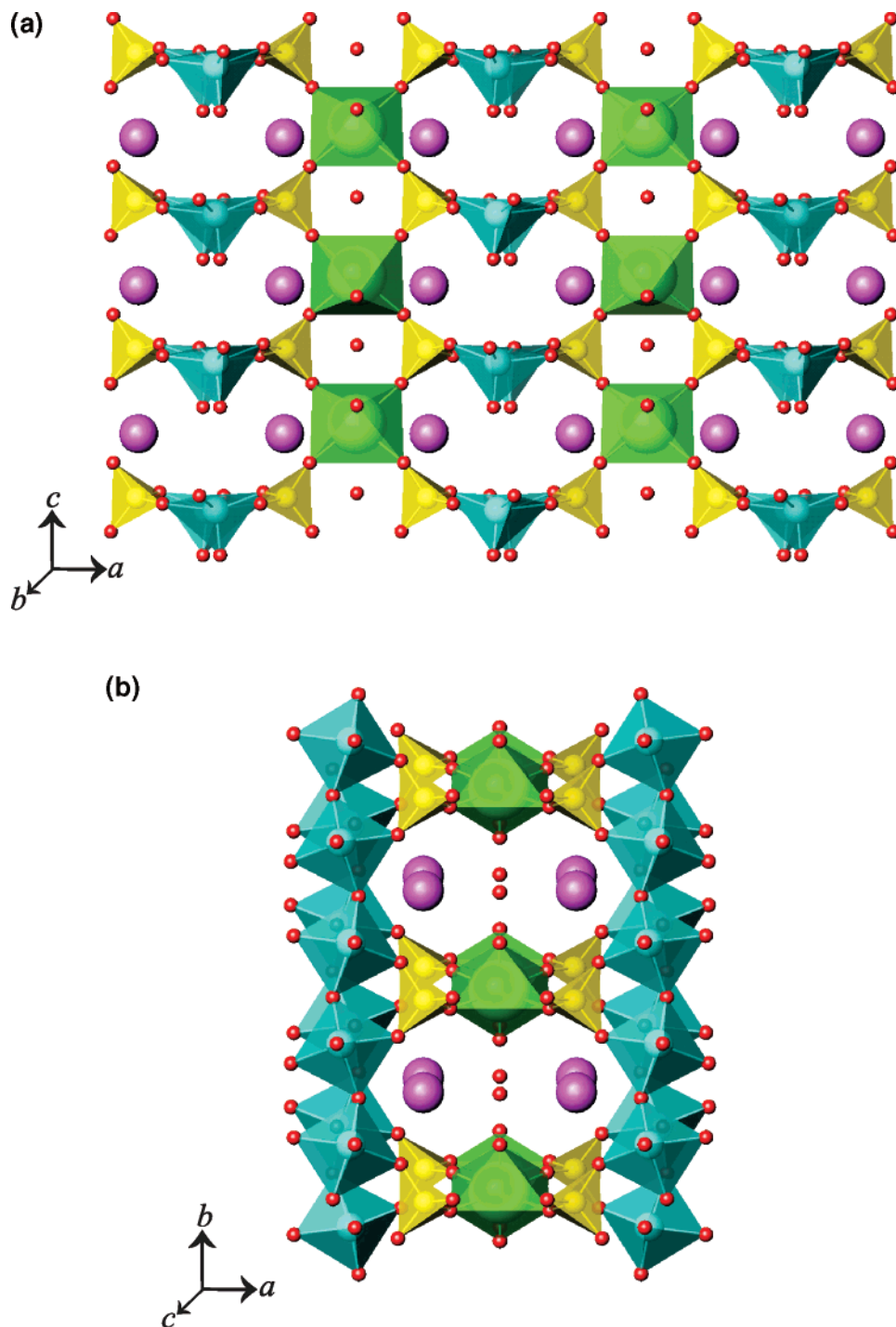


Figure 1. Two views of the structure of $\text{Cs}_2[\text{UO}_2(\text{VO}_2)_2(\text{PO}_4)_2] \cdot 0.59\text{H}_2\text{O}$ (**UVP-1**) that consist of uranyl cations bound by phosphate (shown in yellow) to yield UO_6 tetragonal bipyramids (shown in green). These units are bridged by phosphate to yield one-dimensional chains that run down the c axis. The chains are in turn linked by chains of VO_5 square pyramids (shown in blue) that run down the b axis into an open-framework structure that has intersecting channels that occur along the b (a) and c (b) axes.

features of this structure is that the VO_5 units are oriented so that the single terminal oxo atoms of these polyhedra are all aligned along the c axis as is shown in Figure 1a. **UVP-1** crystallizes in polar orthorhombic space group $Cmc2_1$. As such, c is the polar axis, and the origin of this polarity lies in the alignment of the vanadyl units. The alignment of the vanadyl units is reminiscent of the alignment of titanil units in the key NLO material KTiOPO_4 (KTP).²⁰

The UO_6 units in **UVP-1** display two short $\text{U}=\text{O}$ bond distances of 1.772(7) and 1.781(8) Å, that define the uranyl cation. These bond distances are within the typical range for $\text{U}=\text{O}$ distances.²¹ The lack of imposed inversion symmetry on the uranyl site allows for the observation of both ν_1 and ν_3 modes in the IR at 869 and 886 cm^{-1} , respectively. Longer $\text{U}-\text{O}$ bonds to the equatorial oxygen atoms from the phosphate anions range from 2.250(6) to 2.256(5) Å. These distances were used to calculate a bond-valence sum

(20) (a) Masse, R.; Grenier, J. C. *Bull. Soc. Fr. Mineral. Cristallogr.* **1971**, *94*, 437. (b) Tordjman, I.; Masse, R.; Guitel, J. C. *Z. Kristallogr., Kristallgeom., Kristallphys., Kristallchem.* **1974**, *139*, 103.

(21) Burns, P. C.; Ewing, R. C.; Hawthorne, F. C. *Can. Mineral.* **1997**, *35*, 1551.

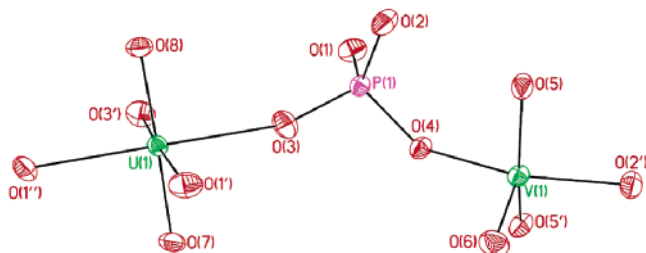


Figure 2. View of the fundamental building units in $\text{Cs}_2[\text{UO}_2(\text{VO}_2)_2(\text{PO}_4)_2] \cdot 0.59\text{H}_2\text{O}$ (**UVP-1**). Fifty percent probability ellipsoids are shown.

for the U center of 6.32, which is consistent with U(VI).²¹ The VO_5 units contain VO_2^+ vanadyl cations with two short $\text{V}=\text{O}$ bonds of 1.600(6) and 1.696(5) Å. The shorter of these bonds is to the terminal oxo atom. The remaining three $\text{V}-\text{O}$ bonds range from 1.921(5) to 1.999(5) Å, yielding a bond-valence sum for the V atom of 5.08.^{22,23} The tetrahedral phosphate anion shows typical $\text{P}-\text{O}$ distances ranging from 1.518(6) to 1.552(6) Å. Finally, the charge balance for the anionic lattice formed by the UO_6 , VO_5 , and PO_4 units is maintained by the Cs^+ cations that form contacts with surrounding oxygen atoms that occur from 3.105(6) to 3.395(6) Å. There are also disordered water molecules with partial occupancy within smaller channels in the structure. There are 0.59 water molecules per formula unit. The fundamental building units in **UVP-1** are shown in Figure 2.

One of the consequences of the polarity in the structure of **UVP-1** is that the compound should exhibit the SHG of laser light; that is, it should act as a NLO material. SHG was investigated using 1064 nm excitation laser pulses from a Q-switched Nd:YAG laser.²⁴ SHG at 532 nm was observed from a polycrystalline sample of **UVP-1**. The response is substantially weaker than that of a commercial ceramic frequency doubling laser beam finder (Kentek View-It). It should also be noted that it is unlikely that a radioactive compound would be used commercially as a NLO material.

It was noted during the course of these studies that some batches of crystals of **UVP-1** had a slightly greenish tint. We speculated that this coloration was due to incomplete oxidation of all of the vanadium sites to V(V) and that trace amounts of V(IV) were present in the samples. Not surprisingly, X-ray diffraction results show virtually identical metrics for both the yellow and the slightly green samples. To test for the presence of V(IV) in the samples we used electron paramagnetic resonance (EPR) spectroscopy (Figure 3).²⁵ In fact, a low concentration of V(IV) sites reduces dipole-dipole interactions and allows for the observation

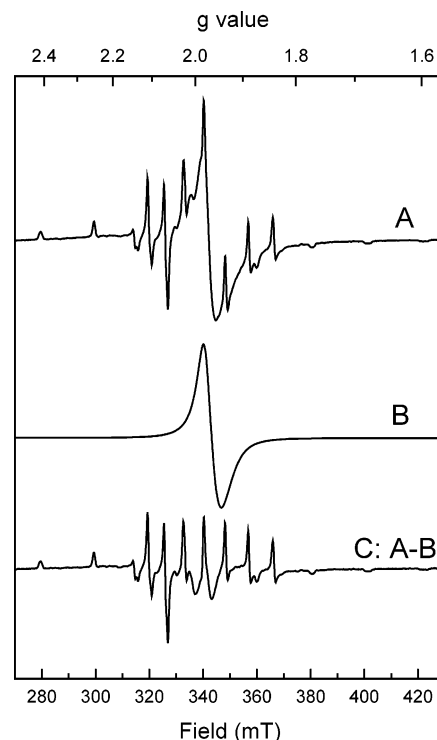


Figure 3. EPR spectra of polycrystalline samples of $\text{Cs}_2[\text{UO}_2(\text{VO}_2)_2(\text{PO}_4)_2] \cdot 0.59\text{H}_2\text{O}$ (**UVP-1**; A) and $\text{Rb}_3\text{Cs}[\text{UO}_2(\text{VO})_4(\text{OH})_2(\text{PO}_4)_4] \cdot n\text{H}_2\text{O}$ (B). Difference spectrum of A and B (C). EPR conditions: microwave frequency, 9434.95 MHz; microwave power, 2.0 mW; modulation amplitude, 0.60 mT; temperature, 298 K.

of relatively sharp signals with hyperfine interactions between the $3d^1$ electron and the ^{51}V nucleus ($I = 7/2$, 99.75%).²⁶ Spectrum A (Figure 3) shows a typical EPR spectrum for a bright yellow-colored sample. This spectrum is a mixture of EPR spectra due to isolated paramagnetic species (sharp peaks) and species that show extensive spin-spin interaction (broad feature) between the paramagnetic species present. The ratio of the broad signal to the sharp signals increases in greenish polycrystalline samples indicating greater spin-spin interactions with increasing V(IV) concentration. This broad feature is similar to that found for the pure V(IV) compound, $\text{Rb}_3\text{Cs}[\text{UO}_2(\text{VO})_4(\text{OH})_2(\text{PO}_4)_4] \cdot n\text{H}_2\text{O}$ (Figure 3B). The spectrum of isolated V(IV) species can be obtained by subtracting the broad EPR spectrum (Figure 3B) from the mixed spectrum (Figure 3A). The resulting EPR spectrum shows the typical eight-line spectrum, consistent with the presence of V(IV) sites within this formally V(V) compound. The line shape of the EPR signal is axial with $g_{xy} > g_z$. Accurate g values could not be obtained due to second-order effects that can mainly be detected as an unequal spacing of the hyperfine lines. The second-order effects can be minimized by measuring at higher frequencies. These measurements are planned for the near future.

There are two potential explanations for the presence of V(IV) sites in **UVP-1**. First, it is possible that there is a slight

(22) Brese, N. E.; O'Keefe, M. *Acta Crystallogr., Sect. B* **1991**, *47*, 192.

(23) Brown, I. D.; Altermatt, D. *Acta Crystallogr., Sect. B* **1985**, *41*, 244.

(24) SHG was investigated using 1064 nm excitation laser pulses from a Q-switched Nd:YAG laser (Continuum Surelite I-10). A Scientech volume absorbing calorimeter was used to measure average laser power. SHG at 532 nm was visually observed in a darkened room from a polycrystalline sample of **UVP-1** contained in a glass tube and was quantified using a band-pass optical filter, IR insensitive photomultiplier (1P28), and a signal averaging digital storage oscilloscope (Tektronix TDS 640A), as the intensity of the unfocused laser beam was increased above the SHG threshold. At a beam cross section averaged intensity of 3.6 MW/cm², the SHG intensity from **UVP-1** was 1500 times weaker than the signal observed from a commercial rare-earth-based ceramic frequency upconverting laser beam finder (Kentek View-It).

(25) EPR spectra at X-band (9.4 GHz) were obtained with a Bruker EMX-6/1 EPR spectrometer composed of the EMX-113 console, ER-041-XG bridge with built-in microwave frequency counter, ER-070 magnet, and ER-4119-HS, high-sensitivity perpendicular-mode cavity. All spectra were recorded with a field modulation frequency of 100 kHz. All samples studied were polycrystalline in nature.

(26) Garces, N. Y.; Stevens, K. T.; Foundos, G. K.; Halliburton, L. E. *J. Phys.: Condens. Matter* **2004**, *16*, 7095.

deficiency in the occupancy of Cs^+ to counterbalance the reduction in positive charge at the vanadium site. This deficiency is not observed in a refinement of the occupancy of the Cs^+ site. Second, it can also be envisioned that protons are introduced into the structure, most likely at the bridging oxide position in the vanadyl phosphate chains. Such protonation occurs in the gallium phosphate chains in the structure of $\text{Cs}_4[(\text{UO}_2)_2(\text{GaOH})_2(\text{PO}_4)_4]\cdot\text{H}_2\text{O}$ (**UGaP-1**).⁶

This work has demonstrated that a remarkable polar mixed-metal uranyl phosphate with an open-framework structure can be prepared under mild hydrothermal conditions. The polarity of the structure allows this compound to display SHG of 532 nm light from a 1064 nm source. A second intriguing feature of this compound is that some of the vanadium can be trapped as V(IV) within the structure, even though this is a formally V(V) compound. Future

reports will detail a series of Ti(III/IV), V(IV), Co(II), and Cu(II) uranyl phosphates that can be isolated from similar reactions.

Acknowledgment. This work was supported by the Chemical Sciences, Geosciences and Biosciences Division, Office of Basic Energy Sciences, Office of Science, Heavy Elements Program, U.S. Department of Energy, under Grant DE-FG02-01ER15187 at Auburn University and under Contract No. W-31-109-ENG-38 at Argonne National Laboratory.

Supporting Information Available: X-ray crystallographic file for $\text{Cs}_2[\text{UO}_2(\text{VO}_2)_2(\text{PO}_4)_2]\cdot 0.59\text{H}_2\text{O}$ (**UVP-1**) in CIF format. This material is available free of charge via the Internet at <http://pubs.acs.org>.

CM052079I